Electronic phase diagram and phase separation in Cr-doped manganites

Y. Moritomo
CIRSE and Department of Crystalline Materials Science, Nagoya University, Nagoya 464-8601, Japan

A. Machida
Department of Crystalline Materials Science, Nagoya University, Nagoya 464-8601, Japan

S. Mori and N. Yamamoto
Department of Physics, Tokyo Institute of Technology, Tokyo 152-8551, Japan

A. Nakamura
CIRSE and Department of Crystalline Materials Science, Nagoya University, Nagoya 464-8601, Japan

(Received 12 January 1999; revised manuscript received 21 May 1999)

Magnetic properties are systematically investigated for Cr-doped manganites $R_{1/2}Ca_{1/2}(Mn,Cr)O_3$ (R=La, Nd, Sm, and Eu) with variation of the averaged ionic radius r_R of the rare-earth ion, or the one-electron bandwidth W. Cr-doping procedure on the perovskite B site significantly unstabilizes the charge-ordered (CO) state, and induces the ferromagnetic metallic (FM) state in the large-r_R($\geqslant$1.29 Å) region. We have found coexistence of the CO domains in the FM phase, or the electronic phase separation, near the FM-CO phase boundary. [S0163-1829(99)08737-8]

Recent extensive study on the perovskite-type doped manganites, which show ''colossal'' magnetoresistance,[1] begins to reveal the unusual microscopical structures of spin-, charge-, and orbital-ordered state.[2–4] The most prototypical example is $La_{1/2}Ca_{1/2}MnO_3$, which is a ferromagnet [T_{CO} ($\sim$190 K)$\leqslant T\leqslant T_C$ (=230 K)] but is transferred into an antiferromagnetic charge-ordered (CO) insulator below T_C.[5] Electron-diffraction measurements[4] on $La_{1/2}Ca_{1/2}MnO_3$ have revealed coexistence of the ferromagnetic metallic (FM) and CO microdomains of order of $\sim$100 nm. In addition, ^{139}La and ^{55}Mn NMR measurements[3] on $La_{1/2}Ca_{1/2}MnO_3$ have confirmed that both the FM and antiferromagnetic CO phases coexist below T_{CO}. Such a coexistence of the FM and CO phases is an interesting aspect of the doped manganites. In the material point of view, $La_{1/2}Ca_{1/2}MnO_3$ locates near the phase boundary between the FM and CO states; $La_{1/2}Sr_{1/2}MnO_3$ with larger one-electron bandwidth W is ferromagnet (T_C=360 K, Ref. 6), while $Pr_{1/2}Ca_{1/2}MnO_3$ with smaller-W shows the charge-ordering transition at T_{CO} =240 K.[7] Then it is plausible that subtle balance of the FM and CO states causes the noble electronic phase separation (PS) in the vicinity of the FM-CO phase boundary.

The generic behavior of paramagnetic-to-ferromagnetic transition of doped manganites is understood within the framework of double-exchange theory,[8–10] which includes only the transfer integral t of the e_g electrons and the on-site exchange interaction (Hund's-rule coupling; J_H) between the itinerant e_g electrons and localized t_{2g} spins (S=3/2). We need to include additional effects, e.g., electron-phonon coupling, however, to understand the insulating behavior in the paramagnetic state.[11] It is well established that the CO state is amenable to the external perturbations, such as, magnetic field,[7,12] external pressure,[13] chemical pressure.[13] In particular, Raveau, Maignan, and Martin[14] have found that substitution of the perovskite B site with other transition metals, e.g., Cr and Co, significantly suppresses the CO phase. Therefore the B-site substitution is the fourth perturbation to control the stability of the CO phase.

In this paper we have investigated the electronic and magnetic properties for Cr-doped manganites $R_{1/2}Ca_{1/2}(Mn,Cr)O_3$ (R=La, Nd, Sm, and Eu) with changing the averaged ionic radius r_R of the rare-earth ion. Here, we can reduce the one-electron bandwidth W by decreasing r_R (*chemical pressure*).[15] Without Cr doping, the ground states of these compounds would be the CO insulating state. We have derived an electronic phase diagram for Cr-doped manganites against r_R (or W), which is dominated by the CO phase in the small-r_R region and the FM phase in the large-r_R region. The magnetization curve in the FM phase is found to be suppressed near the FM-CO phase boundary (1.24 $\leqslant r_R \leqslant$1.27 Å). Dark-field image obtained by electron microscope from a charge-ordering superlattice indicates that the suppression is due to the electronic PS between the CO and FM states.

Ceramics compounds $R_{1/2}Ca_{1/2}(Mn,Cr)O_3$ (R =La, $La_{0.25}Nd_{0.75}$, $La_{0.5}Nd_{0.5}$, $La_{0.75}Nd_{0.25}$, Nd, $Nd_{0.5}Sm_{0.5}$, Sm, and Eu) were synthesized by solid-state reaction in air atmosphere. Stoichiometric mixture of commercial La_2O_3, Nd_2O_3, Sm_2O_3, Eu_2O_3, $CaCO_3$, and Mn_3O_4 powder was well ground and calcined two times at 1250 °C for 24 h. Then the resulting powder was pressed into a disk with a size of 20 mm$\phi\times$4 mm and sintered at 1250 °C for 24 h. Powder x-ray-diffraction measurements at room temperature and Rietveld analysis[16] indicate that both the Cr-undoped and Cr-doped compounds were single phase without detectable impurity. The crystal symmetry is orthorhombic ($Pbnm$; Z=4). We show in Fig. 1 prototypical examples of the x-ray powder patterns together with the best-fitted Rietveld results; upper and lower panels are for $Nd_{1/2}Ca_{1/2}MnO_3$ (R_{wp}=11.16) and

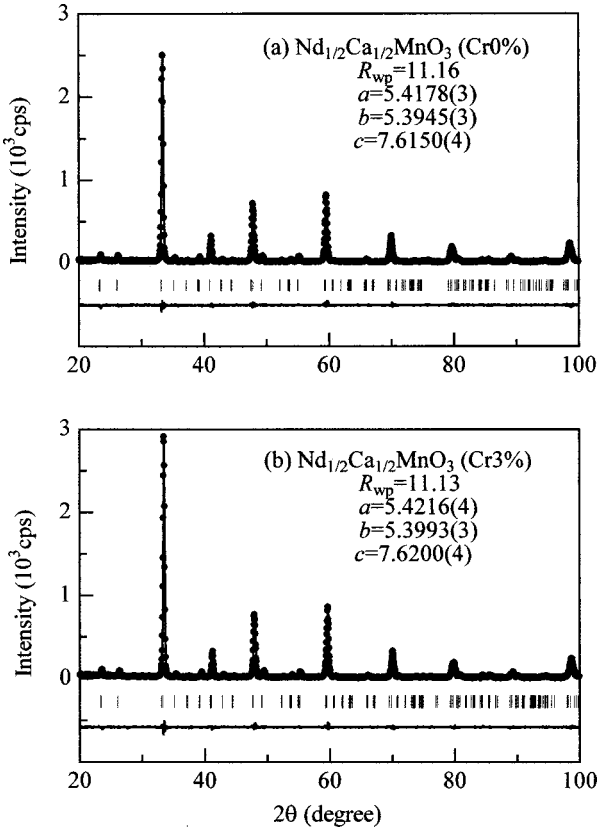

FIG. 1. Powder x-ray pattern (filled circles) for $Nd_{1/2}Ca_{1/2}MnO_3$ (upper panel) and $Nd_{1/2}Ca_{1/2}(Mn_{0.97}Cr_{0.03})O_3$ (lower panel). Solid curve is result of the Rietveld analysis.

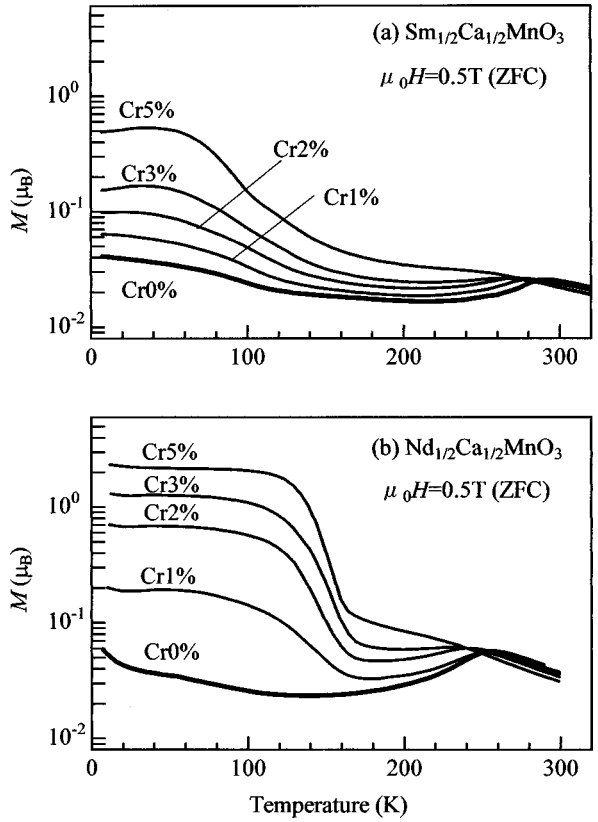

FIG. 2. Cr concentration dependence of magnetization M for (a) $Sm_{1/2}Ca_{1/2}MnO_3$ and (b) $Nd_{1/2}Ca_{1/2}MnO_3$. M was measured after cooling down to 5 K in the zero field (ZFC). Thick curves stand for the Cr-undoped compounds.

$Nd_{1/2}Ca_{1/2}(Mn_{0.97}Cr_{0.03})O_3$ (R_{wp}=11.13), respectively. As seen in the x-ray powder patterns, the quality of the Cr-doped compound is as good as the Cr-undoped one. Lattice constants are determined to be a=5.4178(3) Å, b=5.3945(3) Å, and c=7.6150(4) Å for the Cr-undoped compound. These values slightly increase with Cr-doping to a=5.4216(4) Å, b=5.3993(3) Å, and c=7.6200(4) Å, perhaps reflecting larger ionic radius of Cr^{3+} (=0.61 Å) as compared with Mn^{3+} (=0.59 Å). The lattice structure is nearly cubic; $a \approx b \approx c/\sqrt{2}$. Magnetization M was measured under a field of $\mu_0 H$=0.5 T after cooling down to 5 K in the zero-field cooled (ZFC), using a superconducting quantum interference device (SQUID) magnetometer. For four-probe resistivity measurements, the crystal was cut into a rectangular shape, typically of $3\times2\times1$ mm^3, and electrical contacts were made with a heat-treatment-type silver paint.

Figure 2 shows Cr concentration dependence of mangetization for (a) $Sm_{1/2}Ca_{1/2}MnO_3$ and (b) $Nd_{1/2}Ca_{1/2}MnO_3$. A definite cusp structure, which corresponds to the antiferromagnetic CO transition, is observed at ~280 K (~250 K) for Cr-undoped $Sm_{1/2}Ca_{1/2}MnO_3$ ($Nd_{1/2}Ca_{1/2}MnO_3$). The cusp structure gradually blurred with Cr doping and the M value at lower temperature increases [see Fig. 2(a)]. A drastic effect of the Cr doping is observed in the larger-W system, i.e., $Na_{1/2}Ca_{1/2}MnO_3$ [Fig. 2(b)]. With increases of Cr concentration beyond 2%, the M value steeply rises below ~160 K, showing a ferromagnetic behavior. Such a significant effect has been ascribed to the random effect of the B-site substitution.[17] It is well known that the CO state of doped manganites is accompanied by the alternation of the doubly degenerated e_g orbitals. The B-site randomness destroys the coherence of the orbital and/or charge alternation, and hence makes the ordering short ranged. Katsufuji *et al.*[17] have investigated the microscopic structure of Cr-doped $La_{0.375}Ca_{0.625}MnO_3$ by means of electron microscope, and have found that CO state is of short range with a correlation length of less than 10 nm. (Note that the carrier-doping procedure is qualitatively different from the B-site substitution, because the doped carrier can move and does not destroy the coherence.) On the other hand, the FM state remains long ranged even with the B-site randomness, and has less entropy as compared with the short-ranged CO state. Accordingly, with decrease of temperature, the free energy of the FM state becomes lower than that of the short-ranged CO state.

Now, let us survey the W dependence of the magnetization curve at a fixed Cr-doping level. We show in Fig. 3 temperature dependence of magnetization M of the 3% Cr-doped manganites $R_{1/2}Ca_{1/2}(Mn_{0.97}Cr_{0.03})O_3$. Without the Cr doping, the ground states of these compounds would be antiferromagnetic CO phase with so-called CE-type[18] spin ordering. The M-T curve for $La_{1/2}Ca_{1/2}(Mn_{0.97}Cr_{0.03})O_3$ steeply rises below T_C=240 K (indicated by downward arrow). In the case of R=Sm and Eu, no trace of the ferromagnetic transition is observed in the M-T curve. T_C was determined from the inflection point of the M-T curves. Inset shows the magnetization curve measured at 30 K. The M-H curve of $R=Nd_{0.75}La_{0.25}$ rapidly increases with magnetic field, and reaches $\sim 3\mu_B$ near the ideal value

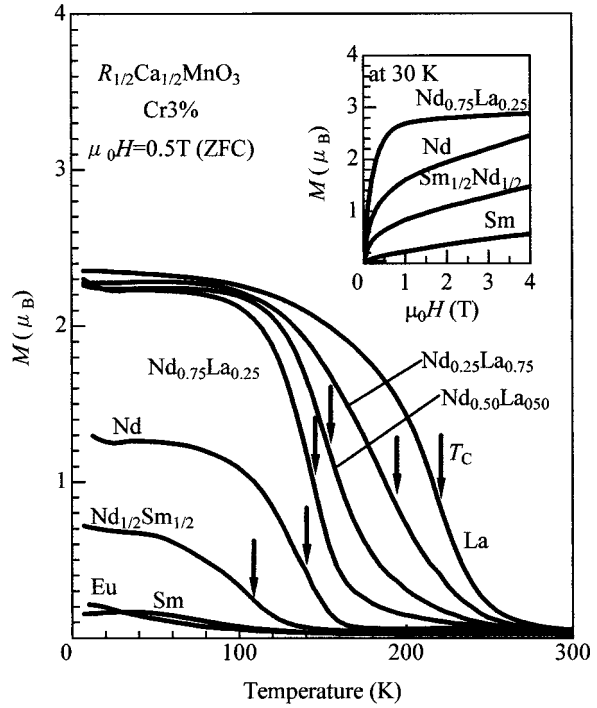

FIG. 3. Temperature dependence of magnetization $M(\mu_B H = 0.5$ T) for 3% Cr-doped manganites $R_{1/2}Ca_{1/2}(Mn_{0.97}Cr_{0.03})O_3$, with variation of the averaged ionic radius r_R of the rare-earth ion. M was measured after cooling down to 5 K in the zero field (ZFC). Arrows indicate the Curie temperatures T_C determined from the infection point of the M-T curves. Inset shows magnetization curves for the Cr-doped manganites.

$(=3.5\mu_B)$ at ~ 1 T. A similar feature of the M-T curve is observed for $R=$La, $Nd_{0.25}La_{0.75}$, and $Nd_{0.5}La_{0.5}$, except for the shift of T_C toward the higher temperature side. The curve for $R=$Sm increases linearly with the applied magnetic field, reflecting the antiferromagnetic CO state.

In the intermediate r_R region, that is, $R=$Nd and $Nd_{0.5}Sm_{0.5}$, a curious magnetic behavior is observed. As seen in Fig. 3, the M-T curve for $R=$Nd $(Nd_{0.5}Sm_{0.5})$ rises at ~ 140 K (~ 110 K), suggesting a paramagnetic-ferromagnetic transition. The magnetization curve shown in the inset, however, increases rather gradually with applied field; M reaches at $\sim 1.6\mu_B$ $(0.8\mu_B)$ at $\mu_0 H=1$ T, and continues to increase up to the highest field ($\mu_0 H=5$ T). Such an $M-H$ behavior is considered to be due to coexistence of antiferromagentic CO domains in the FM state. To confirm this hypothesis, we show in Fig. 4 a dark-field image of $Nd_{1/2}Ca_{1/2}(Mn_{0.97}Cr_{0.03})O_3$ at 120 K. The image is taken using a charge-ordering superlattice reflection (see inset). The CO microdomains with bright contrast are clearly observed in the FM domains with dark contrast.[4] Typical size of the CO microdomains is $\sim 20-50$ nm.

Here, let us argue the e_g-electron density $(1-x)$ of the CO and FM microdomains. The wave vector of the charge ordering is found to be ~ 0.445, indicating that the electron density of the CO microdomain is ~ 0.445 $(x\sim 0.555)$. With use of the nominal electron density $(=0.485)$ of the 3% Cr-doped $Nd_{1/2}Ca_{1/2}MnO_3$, the doping level of the FM microdomain is estimated to be ~ 0.525.[19] In other words, the electron density is slightly dense in the FM microdomain as

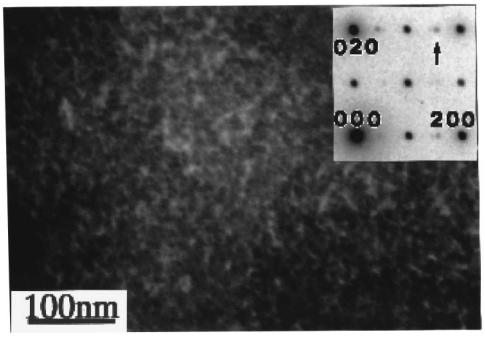

FIG. 4. Dark-field image at 120 K ($\leqslant T_C$) for $Nd_{1/2}Ca_{1/2}(Mn_{0.97}Cr_{0.03})O_3$ obtained from a charge-ordering superlattice reflection (indicated by an arrow in the inset). The bright and dark contrast correspond to the CO and FM microdomains, respectively.

compared with the CO microdomain. Such a *spontaneous* fluctuation of the electron density, or the electronic phase separation (PS), has been theoretically predicted in the doped mangnaites.[2,20] In the actual material, however, the electrostatic energy loss should supress such a density fluctuation. Nevertheless, in the present case, (i) subtle competition between the FM and CO state controlled by chemical pressure as well as (ii) the short-ranged CO state induced by Cr doping seems to stabilize the electronic PS state.

To summarize, we plot in Fig. 5 T_C (filled circles) and the charge-ordering temperature T_{CO} (filled squares) for the Cr-doped $R_{1/2}Ca_{1/2}(Mn_{0.97}Cr_{0.03})O_3$ against r_R. T_{CO} was determined from the maximum point of the activation energy E_{ac} $[=d\ln(\rho)/d(1/T)$, where ρ is resistivity]. The open

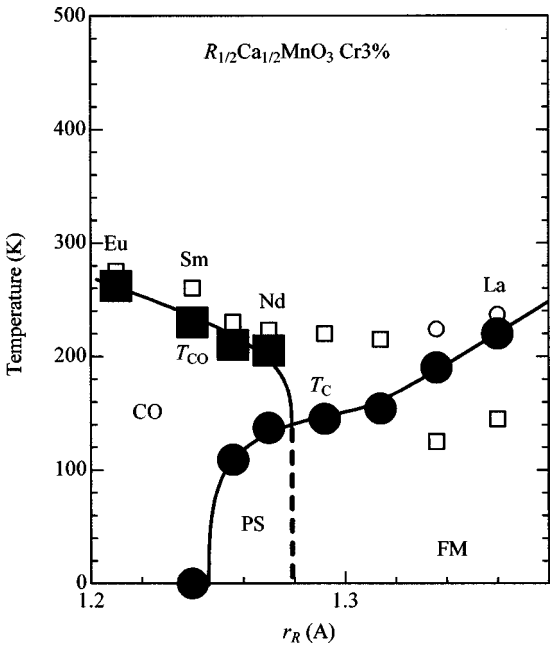

FIG. 5. Electronic phase diagram for 3% Cr-doped manganites $R_{1/2}Ca_{1/2}(Mn_{0.97}Cr_{0.03})O_3$ against averaged ionic radius r_R of the rare-earth ion. Closed circles and squares are Curie temperatures and critical temperatures for the charge-ordering transition, respectively. CO, FM, and CO stand for the charge-ordered, ferromagnetic metallic, and phase separation states, respectively. Open symbols represent the data for the Cr-undoped compounds.

symbols stand for the temperatures for the Cr-undoped compounds. With decrease of r_R, T_C gradually decreases from $T_C \approx 220$ K for $R=$La, and eventually the transition vanishes at $r_R=1.24$ Å ($R=$Sm). Accordingly, T_{CO} appears below $r_R=1.27$ Å($R=$Nd), and then gradually increases up to $T_{CO} \approx 260$ K for $R=$Eu. The electronic PS, which causes the suppressed M-H curve, appears near the FM-CO phase boundary. Thus the electronic PS effect is enhanced in the vicinity of the phase boundary, where two adjacent phases strongly compete.

The authors are grateful to T. Katsufuji for fruitful discussion. This work was supported by a Grant-In-Aid for Scientific Research from the Ministry of Education, Science, Sports and Culture and from Precursory Research for Embryonic Science and Technology (PRESTO), Japan Science and Technology Corporation (JST).

[1] For example, S. Jin, T.H. Tiefel, M. McCormack, R. Fastnacht, R. Ramesh, and L.H. Chen, Science **264**, 13 (1994).
[2] S. Yunoki, J. Hu, A.L. Malvezzi, A. Moreo, N. Furukawa, and E. Dagotto, Phys. Rev. Lett. **80**, 845 (1998).
[3] G. Allodi, R. De Renzi, F. Licci, and M.W. Pieper, Phys. Rev. Lett. **81**, 4736 (1998).
[4] S. Mori, C. H. Chen, and S.-W. Cheong, Phys. Rev. Lett. **81**, 3972 (1998).
[5] P. Schiffer, A.P. Ramirez, W. Bao, and S.-W. Cheong, Phys. Rev. Lett. **75**, 3336 (1998).
[6] Y. Moritomo, T. Akimoto, A. Nakamura, K. Ohoyama, and M. Ohahsi, Phys. Rev. B **58**, 5544 (1998).
[7] Y. Tomioka, A. Asamitsu, H. Kuwahara, Y. Moritomo, and Y. Tokura, Phys. Rev. B **53**, R1689 (1996).
[8] P.W. Anderson and H. Hasagawa, Phys. Rev. **100**, 675 (1955).
[9] P.-G. de Gennes, Phys. Rev. **118**, 141 (1960).
[10] N. Furukawa, J. Phys. Soc. Jpn. **63**, 3214 (1994); **64**, 2734 (1995); **64**, 2754 (1995); **64**, 3164 (1995).
[11] A.J. Millis *et al.*, Phys. Rev. Lett. **74**, 5144 (1995).
[12] H. Kuwahara, Y. Tomioka, A. Asamitsu, Y. Moritomo, and Y. Tokura, Science **270**, 961 (1995).
[13] Y. Moritomo, H. Kuwahara, Y. Tomioka, and Y. Tokura, Phys. Rev. B **55**, 7549 (1997).
[14] B. Raveau, A. Maignan, and C. Martin, J. Solid State Chem. **130**, 162 (1997).
[15] For example, P.G. Radaelli, G. Iannone, M. Marezio, H.-Y. Hwang, S.-W. Cheong, J.D. Jorgensen, and D.N. Argyriou, Phys. Rev. B **56**, 8265 (1997).
[16] F. Izumi, in *The Rietveld Method*, edited by R. A. Young (Oxford University Press, Oxford, 1993), Chap. 13; Y.-I. Kim and F. Izumi, J. Ceram. Soc. Jpn. **102**, 401 (1994).
[17] T. Katsufuji, S.-W. Cheong, S. Mori, and C.-H. Chen, J. Phys. Soc. Jpn. **68**, 1090 (1999).
[18] E.O. Wollan and W.C. Koehler, Phys. Rev. **100**, 545 (1955).
[19] The volume ratio of the FM and CO microdomain in the 3% Cr-doped $Na_{1/2}Ca_{1/2}MnO_3$ is $\sim 1:1$, judging from the magnetization curve.
[20] S. Okamoto, S. Ishihara, and S. Maekawa, cond-mat/9902266 (unpublished).